

Study on the effect of a triple cancer treatment of propolis, thermal cycling-hyperthermia, and low-intensity ultrasound on PANC-1 cells

Yu-Yi Kuo^{1,2}, Wei-Ting Chen^{1,2}, Guan-Bo Lin^{1,2}, Chueh-Hsuan Lu^{1,2}, Chih-Yu Chao^{1,2,3}

¹Department of Physics, Lab for Medical Physics and Biomedical Engineering, National Taiwan University, Taipei, Taiwan

²Molecular Imaging Center, National Taiwan University, Taipei, Taiwan

³Graduate Institute of Applied Physics, Biophysics Division, National Taiwan University, Taipei, Taiwan

Correspondence to: Chih-Yu Chao; email: cychao@phys.ntu.edu.tw

Keywords: combination treatment, synergistic effect, hyperthermia, pancreatic cancer, propolis

Received: February 10, 2023

Accepted: July 6, 2023

Published: July 27, 2023

Copyright: © 2023 Kuo et al. This is an open access article distributed under the terms of the [Creative Commons Attribution License](https://creativecommons.org/licenses/by/3.0/) (CC BY 3.0), which permits unrestricted use, distribution, and reproduction in any medium, provided the original author and source are credited.

ABSTRACT

To reduce side effects and enhance treatment efficacy, study on combination therapy for pancreatic cancer, a deadly cancer, has gained much attraction in recent years. In this study, we propose a novel triple treatment combining propolis and two physical stimuli-thermal cycling-hyperthermia (TC-HT) and low-intensity ultrasound (US). The study found that, after the triple treatment, the cell viability of a human cancer cell line PANC-1 decreased to a level 80% less than the control, without affecting the normal pancreatic cells. Another result was excessive accumulation of reactive oxygen species (ROS) after the triple treatment, leading to the amplification of apoptotic pathway through the MAPK family and mitochondrial dysfunction. This study, to the best of our knowledge, is the first attempt to combine TC-HT, US, and a natural compound in cancer treatment. The combination of TC-HT and US also promotes the anticancer effect of the heat-sensitive chemotherapy drug cisplatin on PANC-1 cells. It is expected that optimized parameters for different agents and different types of cancer will expand the methodology on oncological therapy in a safe manner.

INTRODUCTION

Cancer is one of the most dreadful diseases and the second leading cause of death around the world. Among all cancer types, pancreatic cancer is the most threatening one, due to its high death rate and low five-year survival rate [1]. Existing therapies, including surgery, radiation, and chemotherapy, all involve major risks, such as tumor recurrence, refractory, and serious side effects [2], as a result of which development of new therapies is of the utmost importance. A popular option is combination therapy, administering two or more anticancer agents to attain a synergistic effect [3]. However, drug interactions may lead to unexpected competition and even harmful

side effects [4, 5], jeopardizing patients' health, let alone improving therapeutic efficacy.

An emerging option in combination therapy is physical stimulus, whose effects on cellular physiology have been reported in several studies [6–8]. Our team has looked into the feasibility of combining drug therapy and physical stimuli, such as heat [9], electric field [10], and magnetic field [11]. Ultrasound (US) is another therapeutic tool with extensive application, such as developing internal images [12, 13], transporting liposomes to increase agent-delivery rate [14, 15], and ablating tumors from normal tissues [16, 17]. The previous study also found US as a helpful method in inhibiting the viability of

PANC-1 cells [18]. However, US may also entail risks, such as harm to normal tissues around tumors due to overheating by high-intensity US [19, 20]. In addition, liposomes may induce myocardial injury during transport by US [21, 22]. In view of this, integrating low-intensity US [23, 24] with a non-hazardous agent is important for expanding the use of US in therapy.

Accordingly, the study employed natural compounds from herbal medicines as anticancer agent. Among natural compounds with therapeutic potential, propolis has been found to be effective in inhibiting several cancer cell lines [25–27]. In our previous study, propolis was applied, along with thermal cycling-hyperthermia (TC-HT) as a physical stimulus [28], in cancer treatment, but the effect still lags behind the *in vitro* efficacy of chemotherapy drugs.

In this paper, the study introduced low-intensity US as a secondary helper, on top of TC-HT, in order to further augment the anticancer effect of propolis. The novel triple treatment turned out to inhibit the viability of PANC-1 cells significantly, approaching the *in vitro* efficacy of chemotherapy drugs, without damaging the normal cells. The study found that the low-intensity US in the triple treatment helped to manipulate the phosphorylation levels of mitogen-activated protein kinase (MAPK) family, thereby activating the intracellular apoptotic signalling. Moreover, it was found in the upstream that intracellular reactive oxygen species (ROS) also increased greatly after the low-intensity US was applied in the triple treatment, thereby boosting the death rate of PANC-1 cells.

RESULTS

Triple treatment greatly inhibits the viability of PANC-1 cells

The cell viability of PANC-1 cells versus the propolis concentration was performed in a gradient manner. When the propolis was less than 0.5%, as shown in Figure 1A, there was no notable inhibition effect on 3-(4,5-dimethylthiazol-2-yl)-2,5-diphenyltetrazolium bromide (MTT) results. However, when it exceeded 0.5%, the cell viability dropped significantly. Therefore, a moderate propolis concentration 0.3% was chosen for the following experiments. Next, the physical stimuli of TC-HT and low-intensity US were introduced to affect the viability of PANC-1 cells. In our study, 10-cycles TC-HT and 2.25 MHz US with intensity 0.3 W/cm² and duration 30 minutes were chosen to avoid the thermotoxicity on PANC-1 cells. As shown in Figure 1B, we found that the combination of TC-HT and US was also innocent to PANC-1 cells, but when 0.3% propolis was involved in the triple treatment, the viability of PANC-1 cells was

greatly inhibited. It was also noted that the implementation order of TC-HT and US in triple treatment was influential. When TC-HT was performed prior to US (TC-HT + US) in the presence of 0.3% propolis, US helped to further suppress the cell viability of PANC-1 cells significantly down to 17.1%, cutting more than 80% of the viability of the untreated control and thus approaching the *in vitro* efficacy of chemotherapy drugs. In comparison, the treatment that US was performed prior to TC-HT (US + TC-HT) showed a less inhibition effect (43.1% viability), and hence we adopted the implementation order TC-HT + US as the protocol of the triple treatment in the subsequent experiments. Furthermore, in all double treatments, only 0.3% propolis + TC-HT showed notable inhibition effect (48.9% viability) on PANC-1 cells, which was consistent with our previous results [28]. However, 0.3% propolis + US performed a relatively poor inhibition effect (65.4% viability) on PANC-1 cells, and as a result it was also not included in the following experiments. Figure 1C showed the light microscope images of PANC-1 cells 24 h after each treatment, and the cell morphologies demonstrated an evident inhibition effect on PANC-1 cells after the triple treatment. Moreover, normal cells such as the human skin cells Detroit 551 (Figure 1D) and human pancreatic duct cells H6c7 (Figure 1E) were not significantly affected by the triple treatment as well as all the other treatments. The result indicates that the triple treatment could have a good selective effect on carcinoma cells and normal cells, which makes it safer and more feasible in anticancer treatment.

Triple treatment increases intracellular ROS levels synergistically

Intracellular ROS is an important regulator of cell death. It has been reported that heat and low-intensity US could elevate the intracellular ROS level [29, 30]. We further investigated whether ROS was increased in response to the triple treatment, so the fluorescent dye dihydro-ethidium (DHE) was used in this experiment to determine the level of superoxide radical anion (O₂⁻) in PANC-1 cells after each treatment. As shown in Figure 2A and 2B, it was found that propolis hardly changed the fluorescence signals. Although propolis + TC-HT significantly deformed the fluorescence intensity distribution in an enhanced manner (1.6-fold increase), it did not significantly differ from the enhancement induced by TC-HT alone. In addition, US elevated ROS levels as well, though not as many as TC-HT. Noticeably, the triple treatment showed a significant accumulation of the intracellular ROS (up to a 2.1-fold increase), which was also significantly higher than the TC-HT + 0.3% propolis treatment. The result suggested that, in the triple treatment, US helped to further boost

up the generation of ROS in PANC-1 cells, and could result in enhanced cell death rate after the treatment.

Triple treatment increases mitochondrial apoptosis in PANC-1 cells

It has been known that the enhanced intracellular ROS levels were positively correlated to mitochondrial apopto-

sis [31]. In our work, the apoptotic rates of PANC-1 cells after various treatments were analyzed by the flow cytometry with the fluorescence dye Annexin V and propidium iodide (PI) (Figure 3A and 3B). With the aid of US, the triple treatment further caused 55.3% apoptotic rate, which was significantly higher than the 23.5% apoptotic rate caused by the double treatment of propolis and TC-HT. The cell apoptosis results observed

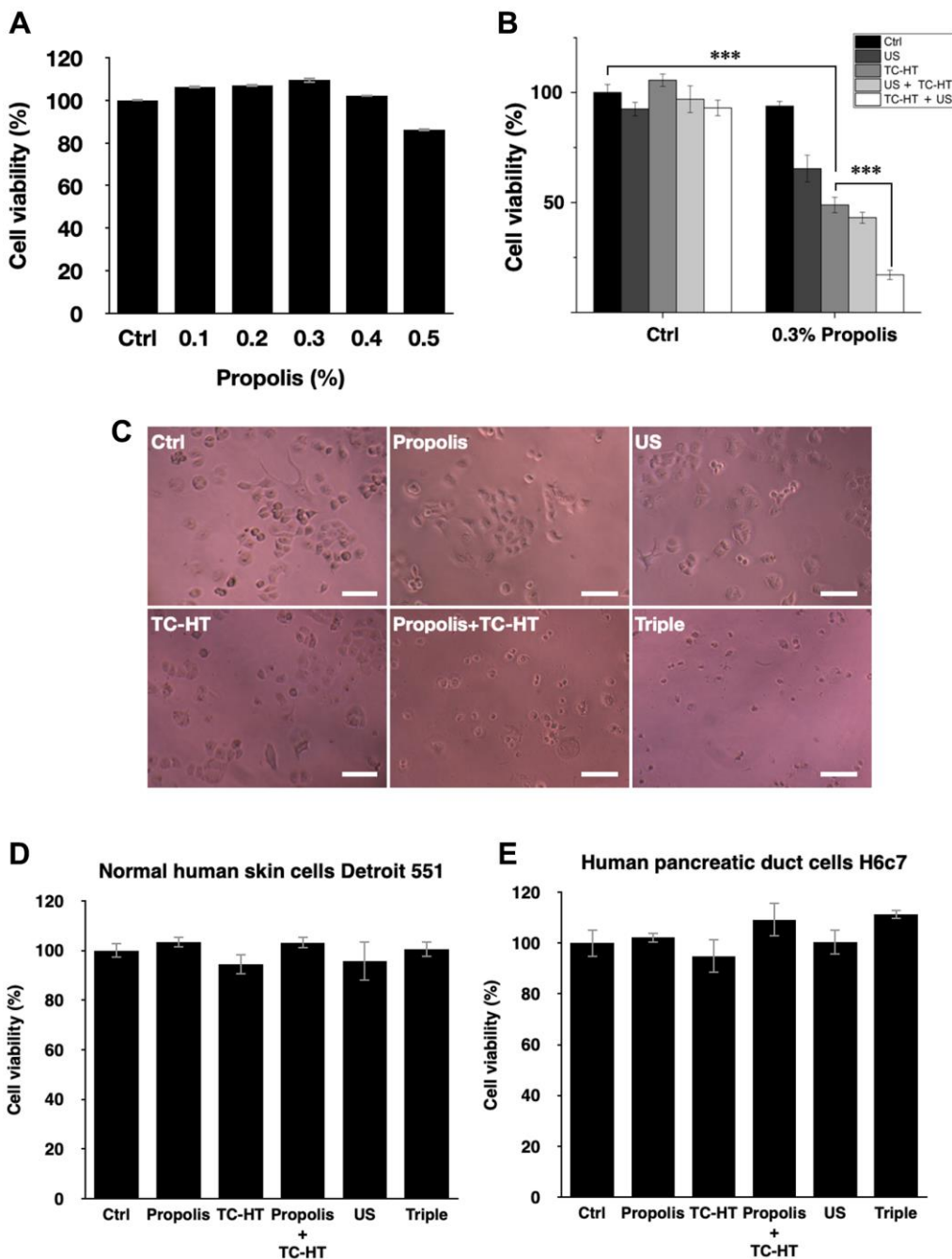


Figure 1. Viability inhibition effects of propolis on PANC-1, Detroit 551, and H6c7 cells. MTT assay was conducted to determine the viabilities of PANC-1 cells after the treatment of (A) different propolis concentrations and (B) different combinations of physical stimulations. (C) Representative light microscope images of PANC-1 cells after each treatment, scale bar = 100 μ m. The viabilities of (D) normal human skin cells Detroit 551 and (E) normal human pancreatic duct cells H6c7 were measured 24 h after each treatment. Data were presented as the mean \pm standard deviation in triplicate. *** $P < 0.001$, comparison between indicated groups.

here were highly consistent with the results of the accumulated ROS levels in PANC-1 cells after the same treatment, as described in Figure 2. Furthermore, the mitochondrial membrane potential (MMP) was assessed using the lipophilic cationic fluorescent dye 3,3'-dihexyloxacarbocyanine iodide (DiOC₆(3)) fluorescence staining by flow cytometric analysis. As shown in Figure 3C and 3D, the ratio of the cells exhibiting MMP loss was significantly promoted to 23.3% after the double treatment of propolis + TC-HT, and it was further elevated significantly to 34.7% by employing the triple treatment. These results showed that adopting US in the triple treatment could decrease MMP level, and hence caused more mitochondrial dysfunction. The decreased MMP level was an indicator of mitochondrial apoptosis, and since the results of apoptosis assay (Figure 3A and 3B) and MMP assay (Figure 3C and 3D) were quite similar, we believe that the mitochondrial dysfunction was implicated in the apoptosis of PANC-1 cells via the triple treatment.

The apoptosis induced by triple treatment is regulated through MAPK pathway

The activation of apoptotic signalling was examined by western blot analysis. As shown in Figure 4A, we

found that the poly (ADP-ribose) polymerase (PARP) cleavage ratio (cleaved PARP/full length PARP), an indicator of caspase-induced apoptosis [32–34], was significantly increased (2.9-fold increase) after propolis + TC-HT treatment on PANC-1 cells. Noticeably, the PARP cleavage was further promoted significantly to a 6.2-fold increase by US in the triple treatment (Figure 4A). Together with the previous flow cytometry results of apoptosis and MMP, it was pointed out that propolis + TC-HT could activate the mitochondrial apoptosis signalling in PANC-1 cells, and US in the triple treatment could further help this cascade to realize a near-chemotherapy level treatment *in vitro*.

Moreover, it was known that the PARP cleavage could be modulated by MMP level, and mitochondrial dysfunction could also be regulated by the excessive intracellular ROS via MAPK family [35]. In MAPK family, the phosphorylated extracellular signal-regulated kinases (p-ERK) level represented the activation of cell survival [36], while the phosphorylated c-Jun N-terminal kinase (p-JNK) and phosphorylated p38 MAPK (p-p38) levels were the indicator of cell death [37, 38]. In this study, it was found that the p-ERK level was suppressed by

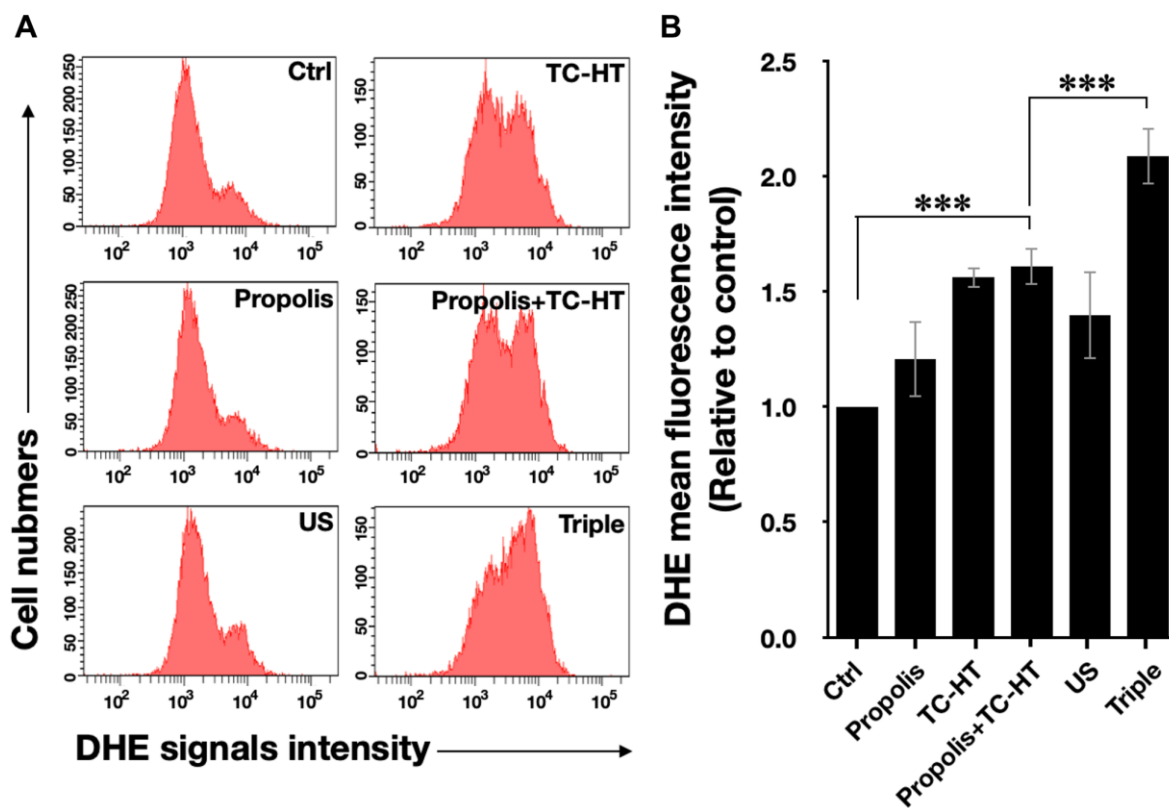


Figure 2. The triple treatment raised the generation of intracellular ROS. (A) Intracellular superoxide radical anion ($O_2^{\cdot -}$) levels of PANC-1 cells were determined by flow cytometry with the fluorescent dye DHE. (B) Quantification of the mean DHE fluorescence levels after each treatment. Data were presented as the mean \pm standard deviation in triplicate. *** $P < 0.001$, comparison between indicated groups.

propolis + TC-HT treatment (0.30-fold decrease), and was further down-regulated when US was introduced in the triple treatment (0.15-fold decrease) (Figure 4B). In addition, the p-JNK and p-p38 levels both exhibited a reverse performance, which were promoted the most in the triple treatment (8.7-fold

and 9.2-fold increase, respectively) (Figure 4C and 4D). These results were consistent with the results of ROS and MMP assessments by flow cytometry. Therefore, we speculated that the excess intracellular ROS induced by the triple treatment regulated the activation of the MAPK family and thus

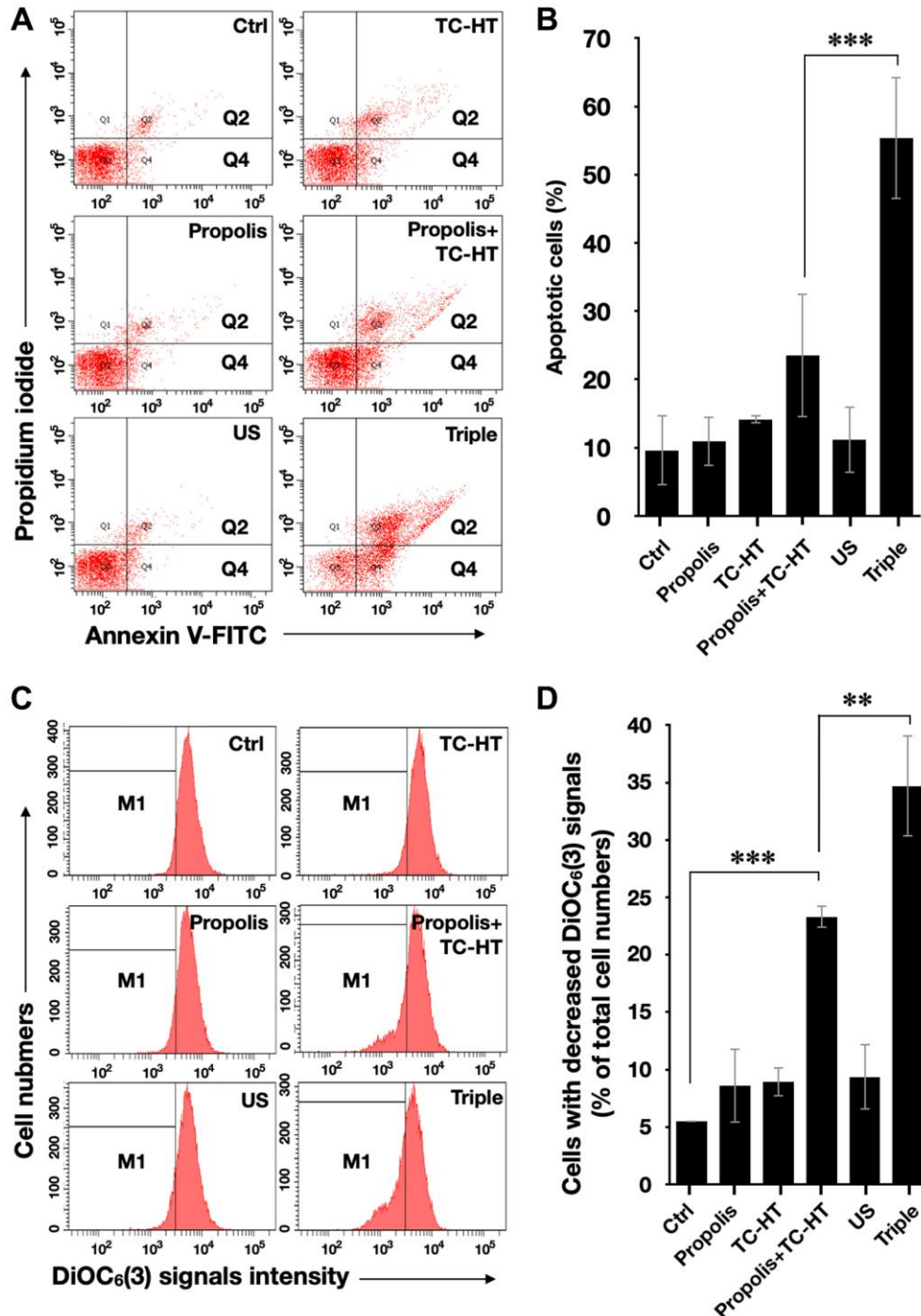


Figure 3. Triple treatment increased apoptosis on PANC-1 cells via mitochondrial dysfunction. (A) Apoptosis after treatment was analyzed via flow cytometry with Annexin V-FITC/PI double staining, and (B) the apoptotic percentage (Q2 + Q4) was calculated. (C) MMP level after treatment was analyzed via flow cytometry with DiOC₆(3) staining, and (D) the percentage of cells with the loss of MMP (M1) was calculated. Data were presented as the mean ± standard deviation in triplicate. ***P* < 0.01, ****P* < 0.001, comparison between indicated groups.

caused mitochondrial dysfunction and the cascade of apoptosis.

ROS scavenger attenuates the apoptosis induced by triple treatment

To further confirm that the cell death after the triple treatment was regulated by the generation of intracellular

ROS, the ROS scavenger N-acetyl-cysteine (NAC) was applied in the experiment [39]. 5 mM NAC was incubated with PANC-1 cells 1 h prior to the triple treatment. As shown in Figure 5A, the inhibitory effect of the triple treatment was restored by NAC, and NAC itself did not affect the viability of PANC-1 cells. Similar results were also observed in the activation of apoptotic pathway, as shown in Figure 5B. NAC alone did not

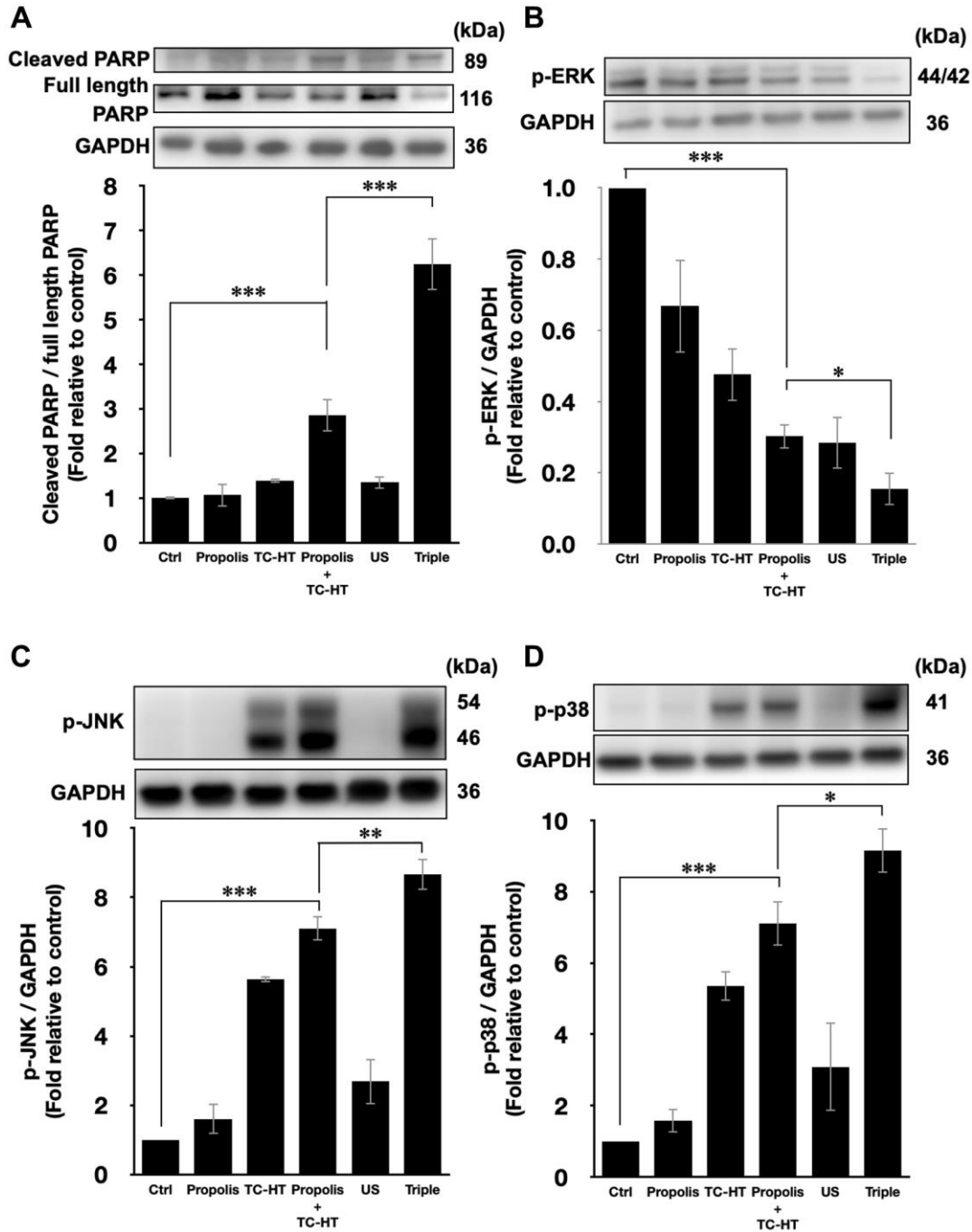


Figure 4. Triple treatment modulated apoptosis via regulating the MAPK family. Representative western blots of the apoptosis-related proteins and the quantification of (A) the PARP cleavage ratio (cleaved PARP/full length PARP), the phosphorylation level of (B) ERK, (C) JNK, and (D) p38. GAPDH was used as loading control. Data were presented as the mean \pm standard deviation in triplicate. * $P < 0.05$, ** $P < 0.01$, *** $P < 0.001$, comparison between indicated groups.

affect PARP cleavage, but it significantly down-regulated the triple treatment-promoted PARP cleavage (Figure 5B). Therefore, the results supported our speculation that the triple treatment could induce mitochondrial apoptosis of PANC-1 cells via the excessive increment of intracellular ROS.

Triple treatment can be applied with chemotherapy drug as a novel anticancer treatment

In this study, we have shown that the method TC-HT followed by mild US exposure could further amplify the anticancer effect of propolis. But, the question is whether the TC-HT + US method can be expanded to the existing chemotherapy drugs. Cisplatin, for instance, was a commonly used clinical chemotherapy drug for several kinds of cancers such as lung, ovarian, breast, and brain cancer [40]. Besides, it has also been reported that cisplatin was sensitive to heat [41]. However, the conventional therapeutic dosage of cisplatin could cause severe side effects to the patients [42, 43], and therefore it was important to develop a new method to reduce the effective dose of cisplatin.

As a result, we applied the method of TC-HT + US with cisplatin on the PANC-1 cells to investigate the potential of this triple treatment method. A relatively low dose of 1 μ M cisplatin and short incubation time 24 h was chosen for the MTT assay independently or in combination with the physical stimulations [44, 45]. After the treatment, the viability of PANC-1 cells was just slightly inhibited by 7.5% by individual cisplatin, and the double treatment of cisplatin + TC-HT also did not alter the viability of PANC-1 cells. The triple treatment, however, promoted the inhibitory effect significantly up to 48.2% (Figure 6A). Moreover, the apoptotic activity was also boosted up by the triple treatment of cisplatin. As shown in Figure 6B, 1 μ M cisplatin alone rarely affected PARP cleavage in PANC-1 cells (0.93-fold decrease), and cisplatin + TC-HT treatment significantly elevated PARP cleavage to a 3.20-fold increase. This elevation was further increased with the help of US (5.82-fold increase). Therefore, compared to the conventional results of cisplatin, our method could not only reduce the effective dose but also boost up the anticancer effect of cisplatin.

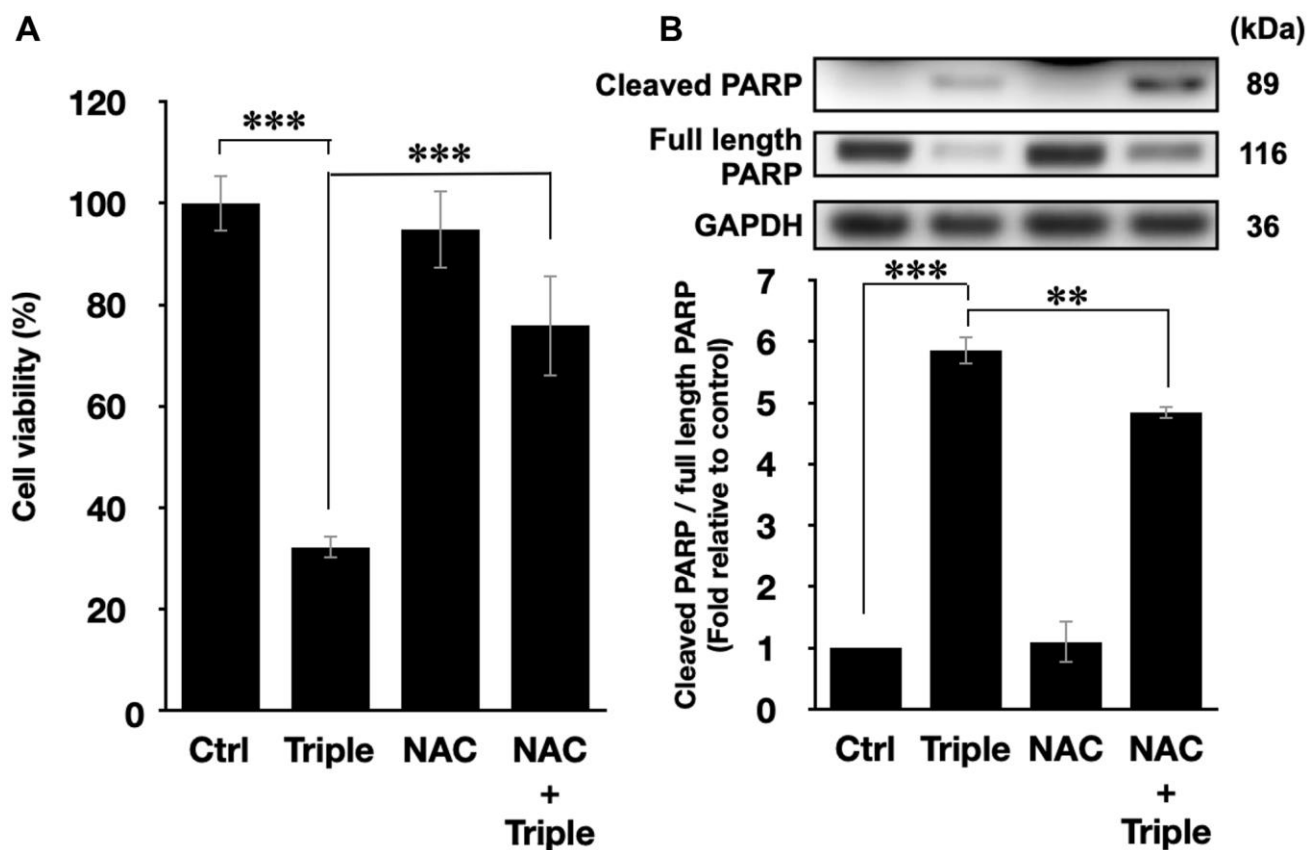


Figure 5. ROS inhibition blocked the cell death and the activation of apoptosis pathways. (A) Cell viabilities of PANC-1 cells and (B) the quantification of PARP cleavage ratio (cleaved PARP/full length PARP) after the triple treatment with or without 1 h NAC pretreatment. GAPDH was used as loading control. Data were presented as the mean \pm standard deviation in triplicate. ** $P < 0.01$, *** $P < 0.001$, comparison between indicated groups.

DISCUSSION

Combination treatment augments the anticancer effect of individual agents by activating multiple pathways, thereby lowering the necessary dosage of the agents to a level harmless to normal cells and human health. However, research on combination anticancer agents is costly and time-consuming [46]. Moreover, unpredictable molecular interactions may be detrimental to patients' health [5]. Therefore, the application of physical stimuli has been considered as a potential candidate for combinative anticancer treatments in combating cancer. Following several combination treatments of physical stimuli and herbal compounds proposed by our team previously [47], the study put forth the combination treatment of propolis, TC-HT, and low-intensity US, proving that it can inhibit pancreatic cancer cell line PANC-1 at a level close to the *in vitro* efficacy of chemotherapy drugs.

In cancer cells, intracellular ROS levels have been known to be the main source of the oxidative stress [48], a key factor for cell viability [49]. Elevated ROS level has been shown to be able to activate some signalling pathways

associated with cell proliferation, apoptosis, and cell cycle progression [50]. Besides, heat treatment and low-intensity US both can increase the intracellular ROS levels [29, 30]. In this work, the study shows that TC-HT significantly augments the intracellular ROS levels of PANC-1 cells (Figure 2A and 2B), at an extent higher than the individual effects of propolis and low-intensity US. It was found that the combination of propolis and TC-HT did not further elevate the levels in PANC-1 cells. Nevertheless, after the low-intensity US was administered, the triple treatment showed a great improvement effect, doubling the intracellular ROS levels of PANC-1 cells. It has been known that excessive intracellular ROS level could activate the apoptotic pathway cascade, increasing the apoptosis in the carcinoma cells [31]. Our study demonstrated that the apoptotic rate of PANC-1 cells was elevated along with the increase of the intracellular ROS levels. The result showed that the triple treatment induced the highest apoptotic rate, compared with other approaches, suggesting its ability to regulate the death of PANC-1 cells via excessive intracellular ROS accumulation. To demonstrate the crucial role of the intracellular ROS levels, NAC was employed in the following experiments

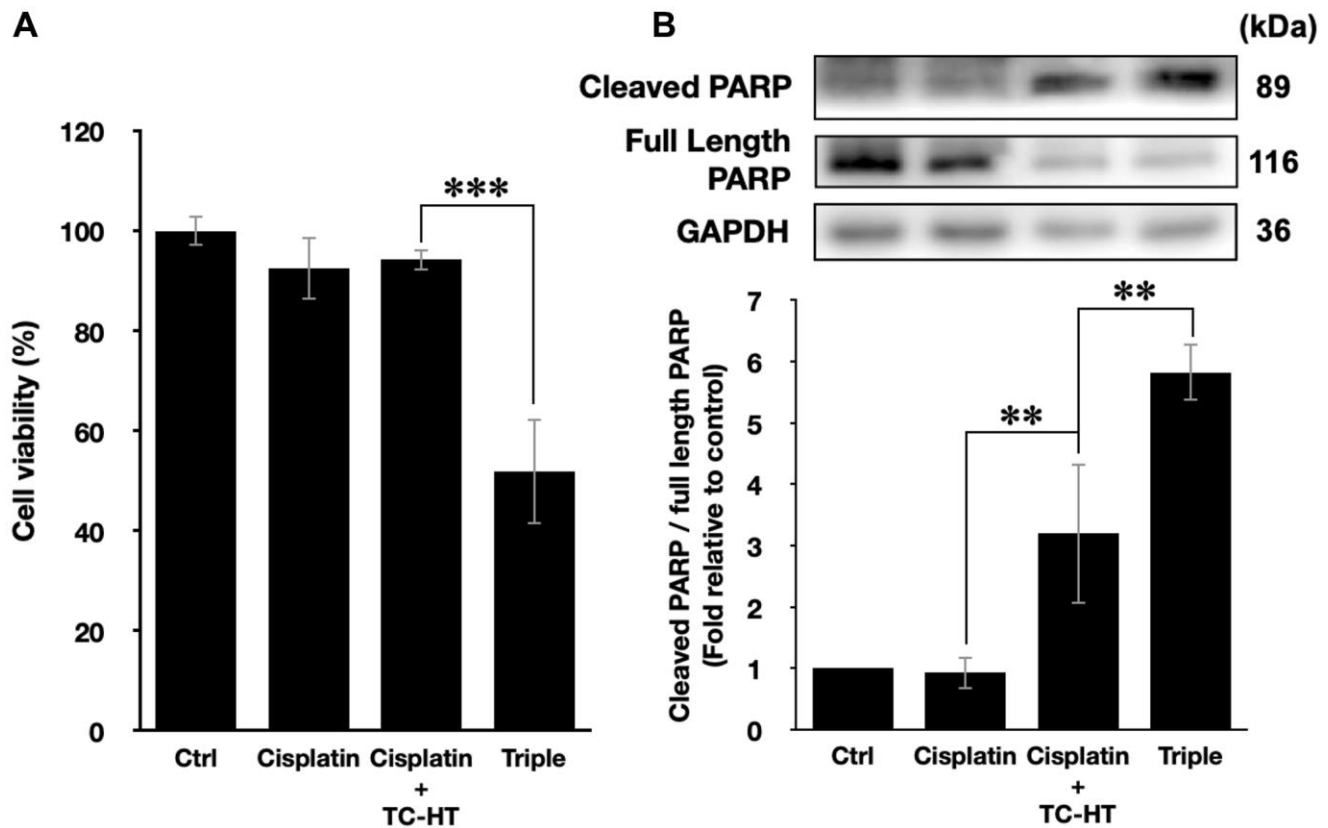


Figure 6. The method of triple treatment promoted the inhibitory effect of the heat sensitive chemotherapy drug cisplatin. (A) Cell viabilities of PANC-1 cells and (B) the quantification of PARP cleavage ratio (cleaved PARP/full length PARP) 24 h after the treatment of cisplatin, cisplatin + TC-HT, and the triple treatment of cisplatin + TC-HT + US. Cisplatin concentrations in all treatments were 1 μ M. Data were presented as the mean \pm standard deviation in triplicate. ** P < 0.01, *** P < 0.001, comparison between indicated groups.

on the triple treatment. While independent NAC pretreatment did not affect the viabilities of PANC-1 cells (Figure 5A), it protected the cells from cytotoxicity in the triple treatment. Hence, ROS elevation played a key role in the anticancer effect in the triple treatment.

The initiation of apoptosis, a common cell death mechanism, is closely related to the function of mitochondria, which is the chemical-energy source of cells and critical for the viability of cells [51]. It was reported that US could induce mitochondrial dysfunction [52], and the dysfunction could induce a series of biochemical cascade of apoptosis, thereby blocking cell proliferation [53]. Meanwhile, the activated members of the MAPK family, such as ERK, JNK, and p38 were deemed to be capable of regulating the dysfunction of mitochondria, and the elevated ROS level was shown to be conducive to the activation of p38 and JNK but down-regulate the activation of ERK [54]. The results suggest that excessive ROS further induced by US could cause greater mitochondrial apoptotic rate via additionally activating the MAPK family members. In this work, our study showed that adopting US in the triple treatment raised greater apoptotic rate of PANC-1 cells (Figure 3A and 3B), while decreasing the MMP level lower, which led to more severe dysfunction of mitochondria than the double treatment of propolis and TC-HT (Figure 3C and 3D). Besides, it has been observed that an active component in propolis could also induce mitochondrial apoptosis in different pancreatic cancer cell line [55]. Furthermore, the mild US in the triple treatment further helped to increase the phosphorylated levels of p38 and JNK significantly, while inhibiting the phosphorylation of ERK (Figure 4), underscoring its ability to manipulate the function of mitochondria via the ROS-activated MAPK family proteins.

The injured mitochondria would release cytochrome-c into the cytoplasm [56], cleaving caspase 9 and thus activating caspase 3 in the downstream [57], which entered further the nucleus and cleaved PARP. Then PARP would lose its enzyme activity, initiating apoptosis irreversibly [58]. In addition, it was reported that US could induce mitochondrial apoptosis in cancer cells [52, 59]. The study demonstrated that the triple treatment could induce mitochondrial dysfunction via regulating the phosphorylation level of the members of MAPK family. In addition, the triple treatment also significantly increased PARP cleavage ratio, an indicator of caspase-induced apoptosis [32–34], compared with the combination treatment of propolis and TC-HT (Figure 4A). This result correlated well with the results of Figures 3 and 4B–4D, suggesting that triple treatment regulated the MAPK family to induce mitochondrial apoptosis. Furthermore, as shown in Figure 5B, it was found that the triple treatment-promoted PARP cleavage

ratio was significantly suppressed by NAC, which indicates that increased ROS level was the key regulator for the apoptotic effect of the triple treatment.

The triple treatment in the study included two physical stimuli, TC-HT and US, which could be integrated for simultaneous implementation via the high-intensity focused ultrasound (HIFU). Being able to raise temperature in the exposed region for energy transfer [19, 20], HIFU has been applied for tumor ablation for over a decade [16, 60]. The temperature increase could be electrically controlled and directed to the targeted region [61]. Therefore, with the help of HIFU, the potential of the triple treatment could be further extended. To augment the applicable value, cisplatin, a common thermal sensitive chemotherapy drug, was incorporated as a substitute for propolis into the triple treatment. It was shown that the inhibited viability of PANC-1 cells by cisplatin was further suppressed with a large extent when both of TC-HT and US were introduced into the treatment (Figure 6A). The dosage of cisplatin can be reduced to a lower concentration, without compromising the anticancer effect. Moreover, the introduction of both physical stimuli further promoted PARP cleavage, indicating that the triple treatment of cisplatin activated more apoptosis in PANC-1 cells (Figure 6B). As a result, the triple treatment has the potential for supplementing the administration of drugs, not only augmenting the effect but also reducing the dosage of the latter. Noteworthy, the apoptotic mechanisms activated by the cisplatin and 0.3% propolis thermal treatments may differ, as indicated by distinct cell viabilities in spite of similar PARP cleavage ratios (Figures 1B, 4A, and 6). This discrepancy might be attributed to cisplatin's ability to mediate PARP cleavage directly through caspase 8 activation, a pathway other than mitochondria dysfunction [62, 63]. Therefore, further studies with other natural compounds or chemotherapy drugs were needed for the investigation of the applicability and the anticancer mechanism of the triple treatment in different kinds of cancer cell lines.

In summary, this study proposed for the first time an effective triple cancer treatment combining propolis, TC-HT, and low-intensity US, which could significantly suppress the growth of PANC-1 cells via an ROS-modulated mitochondrial apoptosis, with a performance comparable to chemotherapy. The study also showed that the triple treatment could induce mitochondrial dysfunction via the regulation of MAPK family, resulting in apoptosis via the up-regulated PARP cleavage. It also demonstrated that the ROS level plays a key role in the performance of the triple treatment. In addition, chemotherapy drugs, such as cisplatin, can be incorporated into the treatment as substitute for propolis. The triple treatment incorporating cisplatin also exhibited a much higher effect in inhibiting cancer cell growth and

cleaving PARP than the cisplatin alone, promising to increase the performance and safety of the existing cancer therapy. Overall, the study proposed employment of physical stimuli, as a promising option in cancer therapy.

MATERIALS AND METHODS

Cell culture and propolis treatment

The human pancreatic cancer cell line PANC-1 and the normal human embryonic skin cell line Detroit 551 were obtained from Bioresource Collection and Research Center (Hsinchu, Taiwan). Normal human pancreatic duct H6c7 cells were purchased from Kerablast, Inc. (Boston, MA, USA). PANC-1 and Detroit 551 cells were cultured respectively in DMEM and EMEM (both from Hyclone, South Logan, UT, USA) supplemented with 10% fetal bovine serum (FBS) (Hyclone) and 1% penicillin-streptomycin (Gibco Life Technologies, Grand Island, NY, USA). H6c7 cells were maintained in keratinocyte-serum free medium (Invitrogen, Life Technologies, Grand Island, NY, USA) supplemented with human recombinant epidermal growth factor, bovine pituitary extract (Invitrogen), and 1% penicillin-streptomycin (Gibco Life Technologies). All cells were maintained in a humidified 5% CO₂ incubator at 37°C and subcultured by 0.05% trypsin–0.5 mM EDTA solution (Gibco Life Technologies). Once the confluences reached suitable percentages, cells were plated in 96-well or 35-mm-diameter culture dishes (Thermo Fisher Scientific, Inc., Waltham, MA, USA) for *in vitro* experiments after 24 h incubation in the humidified 5% CO₂ incubator at 37°C. Propolis was purchased from Grandhealth™ (Grand Health Inc., Richmond, British Columbia, Canada), and cisplatin was obtained from Sigma-Aldrich (St. Louis, MO, USA). All agents were mixed with culture medium to the desired concentration and were incubated with cells for 1 h before treating physical stimuli.

Ultrasound exposure

The US exposure system consisted of a function generator (SG382; Stanford Research Systems, Sunnyvale, CA, USA), a power amplifier (25a250a; Amplifier Research, Souderton, PA, USA), and a planar transducer (A104S-RM; Olympus NDT Inc., Waltham, MA, USA). Continuous pulses were produced using the function generator with the following parameters: -10 dBm amplitude, 1 ms pulse period, and 0.5 ms pulse width. The cell culture plate or dish was placed on the ceramic transducer (resonance frequency 2.25 MHz), which converted electrical signals into acoustic power (Figure 7A). To avoid undesirable thermal effects induced by US, the output power of the spatial average

intensity of the US exposure was adjusted to be 0.3 W/cm² according to the previous studies [64, 65].

Thermal cycling-hyperthermia (TC-HT) treatment

A modified polymerase chain reaction (PCR) system was used to perform TC-HT (Figure 7B). Thermal cycler (model 2720) was purchased from Applied Biosystems (Thermo Fisher Scientific). The system was repeatedly brought to the desired high temperature state and followed by a cooling stage to achieve a series of short period of heat exposure within the desired time (Figure 7C). The experimental setup and administration of TC-HT (10-cycles) have been previously described with optimum results [28]. The actual temperatures the cancer cells sensed were measured by a needle thermocouple, ranging in 45~40.5°C (Figure 7D). Ultrasound exposure was applied either before or after the TC-HT treatment, for different combination tests (Figure 7E). During the TC-HT treatment (~45 min), the control and propolis-treated groups were under room temperature (RT) without a 5% CO₂ environment. No significant impact on cell viability of untreated control cells was observed, regardless of whether the cells were moved outside or placed inside the 5% CO₂ incubator during TC-HT treatment (Supplementary Figure 1). After the treatments, cells were maintained in the cell culture incubator for the following experiments.

MTT assay

MTT (Sigma-Aldrich) was dissolved in distilled water to prepare a 5 mg/mL stock solution. The treated PANC-1 cells were incubated for 4 h in the humidified 5% CO₂ incubator at 37°C with a final MTT concentration 0.5 mg/mL in DMEM culture medium to assess the cell viabilities. The formazan crystals were dissolved by equal volume of the solubilizing buffer of 10% sodium dodecyl sulfate (SDS) (Bioshop Canada Inc., Burlington, Ontario, Canada) solution in 0.01 N hydrochloric acid (HCl) (Echo Chemical Co. Ltd., Miaoli, Taiwan) in the humidified 5% CO₂ incubator at 37°C overnight. The absorbance of each well was detected by Multiskan GO microplate Spectrophotometer (Thermo Fisher Scientific), and the quantity of formazan was determined by the absorbance at 570 nm, with a background subtraction at 690 nm. The cell viabilities were expressed in percentage and the untreated control was set at 100%.

Treatment with ROS scavenger

PANC-1 cells were seeded into 96-well or 35-mm-diameter culture dishes overnight. For ROS inhibition analysis, cells were pretreated with 5 mM NAC (Sigma-Aldrich) in culture medium for 1 h in the humidified 5%

CO₂ incubator at 37°C, and subsequently treated with propolis and/or physical stimuli.

Apoptotic analysis by flow cytometry

PANC-1 cells were collected 24 h after treatments and then rinsed twice with ice-cold phosphate buffered

saline (PBS) (Hyclone). The apoptotic rates were analyzed by the Annexin V-FITC and PI double detection kit (BD Biosciences, San Jose, CA, USA), and the rinsed cells were resuspended in binding buffer containing Annexin V-FITC and PI and then incubated at RT for 15 min in the dark. Apoptotic signals were detected by FACSCanto II system (BD Biosciences).

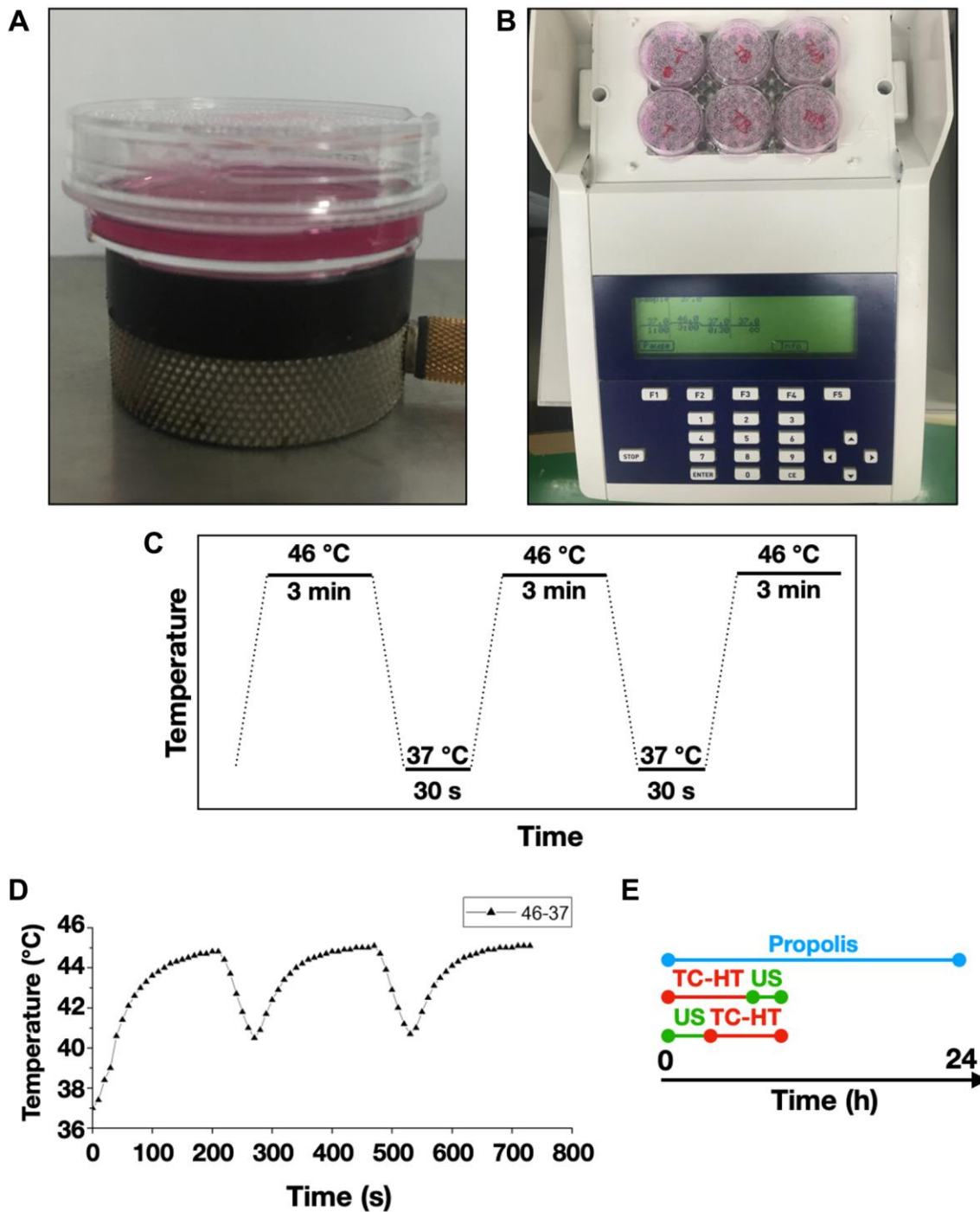


Figure 7. Experimental setups for the triple treatment. 35-mm culture dishes were placed on (A) a ceramic transducer and (B) a modified PCR machine for the exposures of US and TC-HT, respectively. (C) The schematic representation of the TC-HT temperature settings. (D) Cell temperature detected by a needle thermocouple when TC-HT was implemented. (E) Experimental schedule of the triple treatment with different exposing order of US and TC-HT.

ROS and mitochondrial membrane potential (MMP) analyses by flow cytometry

ROS was detected using DHE (Sigma-Aldrich), and the loss of MMP was determined using DiOC₆(3) (Enzo Life Sciences, Inc., Plymouth Meeting, PA, USA). PANC-1 cells were harvested 24 h after treatments and rinsed with PBS before staining. Rinsed cells were resuspended and then incubated with 5 μM DHE or 20 nM DiOC₆(3) in PBS at 37°C for 30 min in the dark. The fluorescence signals were measured by FACSCanto II system (BD Biosciences) with the PE channel (for DHE staining) or FL1 channel (for DiOC₆(3) staining).

Western blot analysis

Protein expression levels of PANC-1 cells were quantified by western blot analysis. Cells were rinsed with PBS and then lysed in the lysis buffer (50 mM Tris-HCl, pH 7.4, 0.15 M NaCl, 0.25% deoxycholic acid, 1% NP-40, 1% Triton X-100, 0.1 % SDS, 1 mM EDTA) (Millipore, Billerica, MA, USA), supplemented with active protease (Millipore) and phosphatase inhibitor cocktail (Cell signaling Technology, Danvers, MA, USA). After centrifugation, the supernatants were collected and the protein concentrations were quantified by Bradford protein assay (Bioshop, Inc.). Equal amount of proteins (20 μg) was resolved by 10% SDS-polyacrylamide gel electrophoresis (SDS-PAGE) and then transferred onto polyvinylidene fluoride (PVDF) membranes (Millipore). 5% skim milk powder or 5% bovine serum albumin in TBST (20 mM Tris-base, pH 7.6, 0.15 M NaCl, 0.1% Tween 20) was used to block nonspecific antibody binding sites for 1 h at RT. Afterwards, the blocked membranes were probed with specific primary antibodies against p-ERK, p-JNK, PARP (Cell signaling), p-p38, and glyceraldehyde-3-phosphate dehydrogenase (GAPDH) (Gentex, Irvine, CA, USA) at 4°C overnight. The membranes were rinsed with TBST buffer three times and then incubated with horseradish peroxidase-conjugated goat anti-rabbit secondary antibodies (Jackson ImmunoResearch Laboratories, West Grove, PA, USA) in a blocking solution at RT for 1 h. Immunoreactivity signal was amplified by an enhanced chemiluminescence (ECL) substrate (Advansta, San Jose, CA, USA) and detected by an imaging system Amersham Imager 600 (GE Healthcare Life Sciences, Chicago, IL, USA). GAPDH was used as the loading control to normalize the relative folds of targeting proteins.

Statistical analysis

Experiments were repeated three times for validation, and statistical analyses were performed using one-way analysis of variance (ANOVA) by OriginPro 2015

software (OriginLab). Results were expressed as the mean ± standard deviation, and were considered to be statistically significant when *P*-values were less than 0.05.

Abbreviations

ANOVA: analysis of variance; DHE: dihydroethidium; DiOC₆(3): 3,3'-dihexyloxacarbocyanine iodide; ECL: enhanced chemiluminescence; FBS: fetal bovine serum; GAPDH: glyceraldehyde-3-phosphate dehydrogenase; HCl: hydrochloric acid; HIFU: high-intensity focused ultrasound; MAPK: mitogen-activated protein kinase; MMP: mitochondrial membrane potential; MTT: 3-(4,5-dimethylthiazol-2-yl)-2,5-diphenyltetrazolium bromide; NAC: N-acetyl-cysteine; O₂^{·-}: superoxide radical anion; p-ERK: phosphorylated extracellular signal-regulated kinases; p-JNK: phosphorylated c-Jun N-terminal kinase; p-p38: phosphorylated p38 MAPK; PARP: poly (ADP-ribose) polymerase; PBS: phosphate buffered saline; PCR: polymerase chain reaction; PI: propidium iodide; PVDF: polyvinylidene fluoride; ROS: reactive oxygen species; SDS: sodium dodecyl sulfate; SDS-PAGE: SDS-polyacrylamide gel electrophoresis; TC-HT: thermal cycling-hyperthermia; US: ultrasound.

AUTHOR CONTRIBUTIONS

C.Y.C. conceived and supervised the study. Y.Y.K., W.T.C. and C.Y.C. designed the study. Y.Y.K. performed experiments and collected data. All authors contributed to data analysis. Y.Y.K. and C.Y.C. wrote the manuscript. All authors contributed to the article and approved the final manuscript.

CONFLICTS OF INTEREST

The authors declare no conflicts of interest related to this study.

FUNDING

This work was supported by grants from Ministry of Science and Technology (MOST 110-2112-M-002-004, MOST 109-2112-M-002-004, and MOST 108-2112-M-002-016 to C.Y.C.) and Ministry of Education (MOE 106R880708 to C.Y.C.) of the Republic of China. The funders had no role in study design, data collection and analysis, decision to publish, or preparation of the manuscript.

REFERENCES

1. Siegel RL, Miller KD, Jemal A. Cancer statistics, 2019. *CA Cancer J Clin.* 2019; 69:7–34. <https://doi.org/10.3322/caac.21551> PMID:30620402

2. Lee JC, Ahn S, Cho IK, Lee J, Kim J, Hwang JH. Management of recurrent pancreatic cancer after surgical resection: a protocol for systematic review, evidence mapping and meta-analysis. *BMJ Open*. 2018; 8:e017249.
<https://doi.org/10.1136/bmjopen-2017-017249>
PMID:[29632079](https://pubmed.ncbi.nlm.nih.gov/29632079/)
3. Yap TA, Omlin A, de Bono JS. Development of therapeutic combinations targeting major cancer signaling pathways. *J Clin Oncol*. 2013; 31:1592–605.
<https://doi.org/10.1200/JCO.2011.37.6418>
PMID:[23509311](https://pubmed.ncbi.nlm.nih.gov/23509311/)
4. Terrault NA. Benefits and risks of combination therapy for hepatitis B. *Hepatology*. 2009; 49:S122–8.
<https://doi.org/10.1002/hep.22921>
PMID:[19399796](https://pubmed.ncbi.nlm.nih.gov/19399796/)
5. Lee JJ, Kong M, Ayers GD, Lotan R. Interaction index and different methods for determining drug interaction in combination therapy. *J Biopharm Stat*. 2007; 17:461–80.
<https://doi.org/10.1080/10543400701199593>
PMID:[17479394](https://pubmed.ncbi.nlm.nih.gov/17479394/)
6. Soares PI, Ferreira IM, Igreja RA, Novo CM, Borges JP. Application of hyperthermia for cancer treatment: recent patents review. *Recent Pat Anticancer Drug Discov*. 2012; 7:64–73.
<https://doi.org/10.2174/157489212798358038>
PMID:[21854362](https://pubmed.ncbi.nlm.nih.gov/21854362/)
7. Davies AM, Weinberg U, Palti Y. Tumor treating fields: a new frontier in cancer therapy. *Ann N Y Acad Sci*. 2013; 1291:86–95.
<https://doi.org/10.1111/nyas.12112>
PMID:[23659608](https://pubmed.ncbi.nlm.nih.gov/23659608/)
8. Wood AKW, Sehgal CM. A review of low-intensity ultrasound for cancer therapy. *Ultrasound Med Biol*. 2015; 41:905–28.
<https://doi.org/10.1016/j.ultrasmedbio.2014.11.019>
PMID:[25728459](https://pubmed.ncbi.nlm.nih.gov/25728459/)
9. Lu CH, Chen WT, Hsieh CH, Kuo YY, Chao CY. Thermal cycling-hyperthermia in combination with polyphenols, epigallocatechin gallate and chlorogenic acid, exerts synergistic anticancer effect against human pancreatic cancer PANC-1 cells. *PLoS One*. 2019; 14:e0217676.
<https://doi.org/10.1371/journal.pone.0217676>
PMID:[31150487](https://pubmed.ncbi.nlm.nih.gov/31150487/)
10. Lu CH, Lin SH, Hsieh CH, Chen WT, Chao CY. Enhanced anticancer effects of low-dose curcumin with non-invasive pulsed electric field on PANC-1 cells. *Oncotargets Ther*. 2018; 11:4723–32.
<https://doi.org/10.2147/OTT.S166264>
PMID:[30127620](https://pubmed.ncbi.nlm.nih.gov/30127620/)
11. Chen WT, Lin GB, Lin SH, Lu CH, Hsieh CH, Ma BL, Chao CY. Static magnetic field enhances the anticancer efficacy of capsaicin on HepG2 cells via capsaicin receptor TRPV1. *PLoS One*. 2018; 13:e0191078.
<https://doi.org/10.1371/journal.pone.0191078>
PMID:[29338036](https://pubmed.ncbi.nlm.nih.gov/29338036/)
12. O'Keeffe D, Mamtora H. Ultrasound in clinical orthopaedics. *J Bone Joint Surg Br*. 1992; 74:488–94.
<https://doi.org/10.1302/0301-620X.74B4.1624502>
PMID:[1624502](https://pubmed.ncbi.nlm.nih.gov/1624502/)
13. Bendick PJ, Brown OW, Hernandez D, Glover JL, Bove PG. Three-dimensional vascular imaging using Doppler ultrasound. *Am J Surg*. 1998; 176:183–7.
[https://doi.org/10.1016/s0002-9610\(98\)00165-2](https://doi.org/10.1016/s0002-9610(98)00165-2)
PMID:[9737629](https://pubmed.ncbi.nlm.nih.gov/9737629/)
14. Ferrara K, Pollard R, Borden M. Ultrasound microbubble contrast agents: fundamentals and application to gene and drug delivery. *Annu Rev Biomed Eng*. 2007; 9:415–47.
<https://doi.org/10.1146/annurev.bioeng.8.061505.095852>
PMID:[17651012](https://pubmed.ncbi.nlm.nih.gov/17651012/)
15. Wang TY, Wilson KE, Machtaler S, Willmann JK. Ultrasound and microbubble guided drug delivery: mechanistic understanding and clinical implications. *Curr Pharm Biotechnol*. 2013; 14:743–52.
<https://doi.org/10.2174/1389201014666131226114611>
PMID:[24372231](https://pubmed.ncbi.nlm.nih.gov/24372231/)
16. Zhou YF. High intensity focused ultrasound in clinical tumor ablation. *World J Clin Oncol*. 2011; 2:8–27.
<https://doi.org/10.5306/wjco.v2.i1.8>
PMID:[21603311](https://pubmed.ncbi.nlm.nih.gov/21603311/)
17. Lang BH, Wu ALH. High intensity focused ultrasound (HIFU) ablation of benign thyroid nodules - a systematic review. *J Ther Ultrasound*. 2017; 5:11.
<https://doi.org/10.1186/s40349-017-0091-1>
PMID:[28523127](https://pubmed.ncbi.nlm.nih.gov/28523127/)
18. Hsieh CH, Lu CH, Kuo YY, Chen WT, Chao CY. Studies on the non-invasive anticancer remedy of the triple combination of epigallocatechin gallate, pulsed electric field, and ultrasound. *PLoS One*. 2018; 13:e0201920.
<https://doi.org/10.1371/journal.pone.0201920>
PMID:[30080905](https://pubmed.ncbi.nlm.nih.gov/30080905/)
19. van den Bijgaart RJ, Eikelenboom DC, Hoogenboom M, Fütterer JJ, den Brok MH, Adema GJ. Thermal and mechanical high-intensity focused ultrasound: perspectives on tumor ablation, immune effects and combination strategies. *Cancer Immunol Immunother*. 2017; 66:247–58.

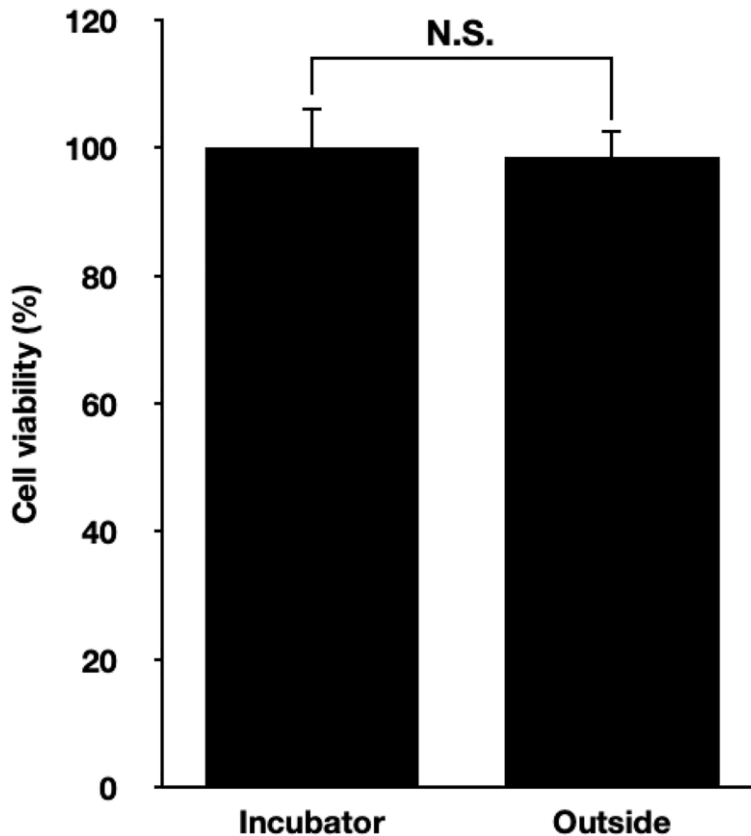
- <https://doi.org/10.1007/s00262-016-1891-9>
PMID:[27585790](https://pubmed.ncbi.nlm.nih.gov/27585790/)
20. Dubinsky TJ, Cuevas C, Dighe MK, Kolokythas O, Hwang JH. High-intensity focused ultrasound: current potential and oncologic applications. *AJR Am J Roentgenol.* 2008; 190:191–9.
<https://doi.org/10.2214/AJR.07.2671>
PMID:[18094311](https://pubmed.ncbi.nlm.nih.gov/18094311/)
21. Zhang B, Zhou H, Cheng Q, Lei L, Hu B. Low-frequency low energy ultrasound combined with microbubbles induces distinct apoptosis of A7r5 cells. *Mol Med Rep.* 2014; 10:3282–8.
<https://doi.org/10.3892/mmr.2014.2654>
PMID:[25324182](https://pubmed.ncbi.nlm.nih.gov/25324182/)
22. Vancraeynest D, Havaux X, Pasquet A, Gerber B, Beauloye C, Rafter P, Bertrand L, Vanoverschelde JL. Myocardial injury induced by ultrasound-targeted microbubble destruction: evidence for the contribution of myocardial ischemia. *Ultrasound Med Biol.* 2009; 35:672–9.
<https://doi.org/10.1016/j.ultrasmedbio.2008.10.005>
PMID:[19110365](https://pubmed.ncbi.nlm.nih.gov/19110365/)
23. Johns LD. Nonthermal effects of therapeutic ultrasound: the frequency resonance hypothesis. *J Athl Train.* 2002; 37:293–9.
PMID:[16558674](https://pubmed.ncbi.nlm.nih.gov/16558674/)
24. Bazou D, Maimon N, Munn LL, Gonzalez I. Effects of low intensity continuous ultrasound (LICU) on mouse pancreatic tumor explants. *Appl Sci.* 2017; 7:1275.
<https://doi.org/10.3390/app7121275>
25. Taira N, Nguyen BC, Be Tu PT, Tawata S. Effect of Okinawa propolis on PAK1 activity, Caenorhabditis elegans longevity, melanogenesis, and growth of cancer cells. *J Agric Food Chem.* 2016; 64:5484–9.
<https://doi.org/10.1021/acs.jafc.6b01785>
PMID:[27337169](https://pubmed.ncbi.nlm.nih.gov/27337169/)
26. Li H, Kapur A, Yang JX, Srivastava S, McLeod DG, Paredes-Guzman JF, Dausgch A, Park YK, Rhim JS. Antiproliferation of human prostate cancer cells by ethanolic extracts of Brazilian propolis and its botanical origin. *Int J Oncol.* 2007; 31:601–6.
<https://doi.org/10.3892/ijo.31.3.601>
PMID:[17671687](https://pubmed.ncbi.nlm.nih.gov/17671687/)
27. Xuan H, Li Z, Yan H, Sang Q, Wang K, He Q, Wang Y, Hu F. Antitumor activity of Chinese propolis in human breast cancer MCF-7 and MDA-MB-231 cells. *Evid Based Complement Alternat Med.* 2014; 2014:280120.
<https://doi.org/10.1155/2014/280120>
PMID:[24963320](https://pubmed.ncbi.nlm.nih.gov/24963320/)
28. Chen WT, Sun YK, Lu CH, Chao CY. Thermal cycling as a novel thermal therapy to synergistically enhance the anticancer effect of propolis on PANC-1 cells. *Int J Oncol.* 2019; 55:617–28.
<https://doi.org/10.3892/ijo.2019.4844>
PMID:[31322205](https://pubmed.ncbi.nlm.nih.gov/31322205/)
29. Hou CH, Lin FL, Hou SM, Liu JF. Hyperthermia induces apoptosis through endoplasmic reticulum and reactive oxygen species in human osteosarcoma cells. *Int J Mol Sci.* 2014; 15:17380–95.
<https://doi.org/10.3390/ijms151017380>
PMID:[25268613](https://pubmed.ncbi.nlm.nih.gov/25268613/)
30. Xia C, Zeng H, Zheng Y. Low-intensity ultrasound enhances the antitumor effects of doxorubicin on hepatocellular carcinoma cells through the ROS-miR-21-PTEN axis. *Mol Med Rep.* 2020; 21:989–98.
<https://doi.org/10.3892/mmr.2020.10936>
PMID:[32016465](https://pubmed.ncbi.nlm.nih.gov/32016465/)
31. Redza-Dutordoir M, Averill-Bates DA. Activation of apoptosis signalling pathways by reactive oxygen species. *Biochim Biophys Acta.* 2016; 1863:2977–92.
<https://doi.org/10.1016/j.bbamcr.2016.09.012>
PMID:[27646922](https://pubmed.ncbi.nlm.nih.gov/27646922/)
32. Jiang L, Xu K, Li J, Zhou X, Xu L, Wu Z, Ma C, Ran J, Hu P, Bao J, Wu L, Xiong Y. Nesfatin-1 suppresses interleukin-1 β -induced inflammation, apoptosis, and cartilage matrix destruction in chondrocytes and ameliorates osteoarthritis in rats. *Aging (Albany NY).* 2020; 12:1760–77.
<https://doi.org/10.18632/aging.102711>
PMID:[32003758](https://pubmed.ncbi.nlm.nih.gov/32003758/)
33. Fukuta K, Kohri K, Fukuda H, Watanabe M, Sugimura T, Nakagama H. Induction of multinucleated cells and apoptosis in the PC-3 prostate cancer cell line by low concentrations of polyethylene glycol 1000. *Cancer Sci.* 2008; 99:1055–62.
<https://doi.org/10.1111/j.1349-7006.2008.00781.x>
PMID:[18380794](https://pubmed.ncbi.nlm.nih.gov/18380794/)
34. Subramanian A, Andronache A, Li YC, Wade M. Inhibition of MARCH5 ubiquitin ligase abrogates MCL1-dependent resistance to BH3 mimetics via NOXA. *Oncotarget.* 2016; 7:15986–6002.
<https://doi.org/10.18632/oncotarget.7558>
PMID:[26910119](https://pubmed.ncbi.nlm.nih.gov/26910119/)
35. Zang YQ, Feng YY, Luo YH, Zhai YQ, Ju XY, Feng YC, Sheng YN, Wang JR, Yu CQ, Jin CH. Quinalizarin induces ROS-mediated apoptosis via the MAPK, STAT3 and NF- κ B signaling pathways in human breast cancer cells. *Mol Med Rep.* 2019; 20:4576–86.
<https://doi.org/10.3892/mmr.2019.10725>
PMID:[31702038](https://pubmed.ncbi.nlm.nih.gov/31702038/)
36. Meng J, Fang B, Liao Y, Chresta CM, Smith PD, Roth JA. Apoptosis induction by MEK inhibition in human lung cancer cells is mediated by Bim. *PLoS One.* 2010; 5:e13026.

- <https://doi.org/10.1371/journal.pone.0013026>
PMID:20885957
37. Chiyo T, Fujita K, Iwama H, Fujihara S, Tadokoro T, Ohura K, Matsui T, Goda Y, Kobayashi N, Nishiyama N, Yachida T, Morishita A, Kobara H, et al. Galectin-9 induces mitochondria-mediated apoptosis of esophageal cancer in vitro and in vivo in a xenograft mouse model. *Int J Mol Sci.* 2019; 20:2634.
<https://doi.org/10.3390/ijms20112634>
PMID:31146370
38. Wu YJ, Su TR, Dai GF, Su JH, Liu CI. Flaccidoxide-13-acetate-induced apoptosis in human bladder cancer cells is through activation of p38/JNK, mitochondrial dysfunction, and endoplasmic reticulum stress regulated pathway. *Mar Drugs.* 2019; 17:287.
<https://doi.org/10.3390/md17050287>
PMID:31086026
39. Aruoma OI, Halliwell B, Hoey BM, Butler J. The antioxidant action of N-acetylcysteine: its reaction with hydrogen peroxide, hydroxyl radical, superoxide, and hypochlorous acid. *Free Radic Biol Med.* 1989; 6:593–7.
[https://doi.org/10.1016/0891-5849\(89\)90066-x](https://doi.org/10.1016/0891-5849(89)90066-x)
PMID:2546864
40. Dasari S, Tchounwou PB. Cisplatin in cancer therapy: molecular mechanisms of action. *Eur J Pharmacol.* 2014; 740:364–78.
<https://doi.org/10.1016/j.ejphar.2014.07.025>
PMID:25058905
41. Behrouzkhia Z, Joveini Z, Keshavarzi B, Eyvazzadeh N, Aghdam RZ. Hyperthermia: how can it be used? *Oman Med J.* 2016; 31:89–97.
<https://doi.org/10.5001/omj.2016.19>
PMID:27168918
42. Florea AM, Büsselberg D. Cisplatin as an anti-tumor drug: cellular mechanisms of activity, drug resistance and induced side effects. *Cancers (Basel).* 2011; 3:1351–71.
<https://doi.org/10.3390/cancers3011351>
PMID:24212665
43. Ghosh S. Cisplatin: the first metal based anticancer drug. *Bioorg Chem.* 2019; 88:102925.
<https://doi.org/10.1016/j.bioorg.2019.102925>
PMID:31003078
44. Cregan IL, Dharmarajan AM, Fox SA. Mechanisms of cisplatin-induced cell death in malignant mesothelioma cells: role of inhibitor of apoptosis proteins (IAPs) and caspases. *Int J Oncol.* 2013; 42:444–52.
<https://doi.org/10.3892/ijo.2012.1715>
PMID:23229133
45. Beer M, Kuppalu N, Stefanini M, Becker H, Schulz I, Manoli S, Schuette J, Schmees C, Casazza A, Stelzle M, Arcangeli A. A novel microfluidic 3D platform for culturing pancreatic ductal adenocarcinoma cells: comparison with in vitro cultures and in vivo xenografts. *Sci Rep.* 2017; 7:1325.
<https://doi.org/10.1038/s41598-017-01256-8>
PMID:28465513
46. Huang H, Zhang P, Qu XA, Sanseau P, Yang L. Systematic prediction of drug combinations based on clinical side-effects. *Sci Rep.* 2014; 4:7160.
<https://doi.org/10.1038/srep07160>
PMID:25418113
47. Lu CH, Kuo YY, Lin GB, Chen WT, Chao CY. Application of non-invasive low-intensity pulsed electric field with thermal cycling-hyperthermia for synergistically enhanced anticancer effect of chlorogenic acid on PANC-1 cells. *PLoS One.* 2020; 15:e0222126.
<https://doi.org/10.1371/journal.pone.0222126>
PMID:31995555
48. Liou GY, Storz P. Reactive oxygen species in cancer. *Free Radic Res.* 2010; 44:479–96.
<https://doi.org/10.3109/10715761003667554>
PMID:20370557
49. Kannan K, Jain SK. Oxidative stress and apoptosis. *Pathophysiology.* 2000; 7:153–63.
[https://doi.org/10.1016/s0928-4680\(00\)00053-5](https://doi.org/10.1016/s0928-4680(00)00053-5)
PMID:10996508
50. Aggarwal V, Tuli HS, Varol A, Thakral F, Yerer MB, Sak K, Varol M, Jain A, Khan MA, Sethi G. Role of reactive oxygen species in cancer progression: molecular mechanisms and recent advancements. *Biomolecules.* 2019; 9:735.
<https://doi.org/10.3390/biom9110735>
PMID:31766246
51. Osellame LD, Blacker TS, Duchon MR. Cellular and molecular mechanisms of mitochondrial function. *Best Pract Res Clin Endocrinol Metab.* 2012; 26:711–23.
<https://doi.org/10.1016/j.beem.2012.05.003>
PMID:23168274
52. Wang P, Leung AW, Xu C. Low-intensity ultrasound-induced cellular destruction and autophagy of nasopharyngeal carcinoma cells. *Exp Ther Med.* 2011; 2:849–52.
<https://doi.org/10.3892/etm.2011.317>
PMID:22977587
53. Elmore S. Apoptosis: a review of programmed cell death. *Toxicol Pathol.* 2007; 35:495–516.
<https://doi.org/10.1080/01926230701320337>
PMID:17562483
54. Yuan L, Wang J, Xiao H, Wu W, Wang Y, Liu X. MAPK signaling pathways regulate mitochondrial-mediated

- apoptosis induced by isoorientin in human hepatoblastoma cancer cells. *Food Chem Toxicol.* 2013; 53:62–8.
<https://doi.org/10.1016/j.fct.2012.11.048>
PMID:[23220614](https://pubmed.ncbi.nlm.nih.gov/23220614/)
55. Chen MJ, Chang WH, Lin CC, Liu CY, Wang TE, Chu CH, Shih SC, Chen YJ. Caffeic acid phenethyl ester induces apoptosis of human pancreatic cancer cells involving caspase and mitochondrial dysfunction. *Pancreatology.* 2008; 8:558–65.
<https://doi.org/10.1159/000159214>
PMID:[18824880](https://pubmed.ncbi.nlm.nih.gov/18824880/)
56. Garrido C, Galluzzi L, Brunet M, Puig PE, Didelot C, Kroemer G. Mechanisms of cytochrome c release from mitochondria. *Cell Death Differ.* 2006; 13:1423–33.
<https://doi.org/10.1038/sj.cdd.4401950>
PMID:[16676004](https://pubmed.ncbi.nlm.nih.gov/16676004/)
57. Brentnall M, Rodriguez-Menocal L, De Guevara RL, Cepero E, Boise LH. Caspase-9, caspase-3 and caspase-7 have distinct roles during intrinsic apoptosis. *BMC Cell Biol.* 2013; 14:32.
<https://doi.org/10.1186/1471-2121-14-32>
PMID:[23834359](https://pubmed.ncbi.nlm.nih.gov/23834359/)
58. Jimenez F, Aiba-Masago S, Al Hashimi I, Vela-Roch N, Fernandes G, Yeh CK, Talal N, Dang H. Activated caspase 3 and cleaved poly(ADP-ribose)polymerase in salivary epithelium suggest a pathogenetic mechanism for Sjögren's syndrome. *Rheumatology (Oxford).* 2002; 41:338–42.
<https://doi.org/10.1093/rheumatology/41.3.338>
PMID:[11934973](https://pubmed.ncbi.nlm.nih.gov/11934973/)
59. Feng Y, Tian Z, Wan M. Bioeffects of low-intensity ultrasound in vitro: apoptosis, protein profile alteration, and potential molecular mechanism. *J Ultrasound Med.* 2010; 29:963–74.
<https://doi.org/10.7863/jum.2010.29.6.963>
PMID:[20498470](https://pubmed.ncbi.nlm.nih.gov/20498470/)
60. Duc NM, Keserci B. Emerging clinical applications of high-intensity focused ultrasound. *Diagn Interv Radiol.* 2019; 25:398–409.
<https://doi.org/10.5152/dir.2019.18556>
PMID:[31287428](https://pubmed.ncbi.nlm.nih.gov/31287428/)
61. Park S, Pham NT, Huynh HT, Kang HW. Development of temperature controller-integrated portable HIFU driver for thermal coagulation. *Biomed Eng Online.* 2019; 18:77.
<https://doi.org/10.1186/s12938-019-0697-3>
PMID:[31242902](https://pubmed.ncbi.nlm.nih.gov/31242902/)
62. Mohiuddin M, Kasahara K. Cisplatin activates the growth inhibitory signaling pathways by enhancing the production of reactive oxygen species in non-small cell lung cancer carrying an EGFR exon 19 deletion. *Cancer Genomics Proteomics.* 2021; 18:471–86.
<https://doi.org/10.21873/cgp.20273>
PMID:[33994369](https://pubmed.ncbi.nlm.nih.gov/33994369/)
63. Paul I, Chacko AD, Stasik I, Busacca S, Crawford N, McCoy F, McTavish N, Wilson B, Barr M, O'Byrne KJ, Longley DB, Fennell DA. Acquired differential regulation of caspase-8 in cisplatin-resistant non-small-cell lung cancer. *Cell Death Dis.* 2012; 3:e449.
<https://doi.org/10.1038/cddis.2012.186>
PMID:[23254292](https://pubmed.ncbi.nlm.nih.gov/23254292/)
64. Love L, Kremkau F. Intracellular temperature distribution produced by ultrasound. *J Acoust Soc Am.* 1980; 67:1045–50.
<https://doi.org/10.1121/1.384072>
65. Nahirnyak V, Mast TD, Holland CK. Ultrasound-induced thermal elevation in clotted blood and cranial bone. *Ultrasound Med Biol.* 2007; 33:1285–95.
<https://doi.org/10.1016/j.ultrasmedbio.2007.02.005>
PMID:[17490808](https://pubmed.ncbi.nlm.nih.gov/17490808/)

SUPPLEMENTARY MATERIALS

Supplementary Figure



Supplementary Figure 1. Comparison of viabilities of untreated control PANC-1 cells inside or outside the incubator during TC-HT treatment (~45 min). MTT assay was conducted to determine the viabilities of PANC-1 cells after 24 h incubation. Data were presented as the mean ± standard deviation ($n = 4$). N.S. denotes a statistically non-significant difference within the indicated group.